Science

AAAS

The Impact of Agricultural Soil Erosion on the Global Carbon Cycle

K. Van Oost, *et al.*
Science **318**, 626 (2007);
DOI: 10.1126/science.1145724

Earth's upper mantle related to large-scale convective processes.

References and Notes

1. P. M. Shearer, *J. Geophys. Res.* **96**, 18147 (1991).
2. Y. Fei *et al.*, *J. Geophys. Res.* **109**, 10.1029/2003JB002562 (2004).
3. M. Akaogi, E. Ito, A. Navrotsky, *J. Geophys. Res.* **94**, 15671 (1989).
4. E. Ito, E. Takahashi, *J. Geophys. Res.* **94**, 10637 (1989).
5. M. P. Flanagan, P. M. Shearer, *J. Geophys. Res.* **103**, 2673 (1998).
6. J. Gossler, R. Kind, *Earth Planet. Sci. Lett.* **138**, 1 (1996).
7. Y. J. Gu, A. M. Dziewonski, *J. Geophys. Res.* **107**, 2135 (2002).
8. S. Lebedev, S. Chevrot, R. D. van der Hilst, *Science* **296**, 1300 (2002).
9. K. H. Liu, S. S. Gao, P. G. Silver, Y. K. Zhang, *J. Geophys. Res.* **108**, 10.1029/2002JB002208 (2003).
10. J. D. Collier, G. R. Helffrich, *Geophys. J. Int.* **147**, 319 (2001).
11. M. P. Flanagan, P. M. Shearer, *J. Geophys. Res.* **103**, 21165 (1998).
12. N. Schmerr, E. Garnero, *J. Geophys. Res.* **111**, 10.1029/2005JB004197 (2006).
13. Materials and methods are available as supporting material on *Science* online.
14. B. Efron, R. Tibshirani, *Stat. Sci.* **1**, 54 (1986).
15. A. Deuss, S. A. T. Redfern, K. Chambers, J. H. Woodhouse, *Science* **311**, 198 (2006).
16. Y. C. Zheng, T. Lay, M. P. Flanagan, Q. Williams, *Science* **316**, 855 (2007).
17. N. A. Simmons, H. Gurrola, *Nature* **405**, 559 (2000).
18. C. R. Bina, B. J. Wood, *J. Geophys. Res.* **92**, 4853 (1987).
19. L. Stixrude, *J. Geophys. Res.* **102**, 14835 (1997).
20. J. R. Smyth, S. D. Jacobsen, in *Earth's Deep Water Cycle*, S. D. Jacobsen, S. Van der Lee, Eds. (American Geophysical Union, Washington, DC, 2006), vol. 168, pp. 1–11.
21. M. M. Hirschmann, *Annu. Rev. Earth Planet. Sci.* **34**, 629 (2006).
22. S. Karato, in *Water in Nominally Anhydrous Minerals*, H. Keppler, J. R. Smyth, Eds. (Geochemical Society, St. Louis, MO, 2006), vol. 62, pp. 343–375.
23. G. M. Leahy, D. Bercovici, *J. Geophys. Res.* **112**, 10.1029/2006JB004631 (2007).
24. Y. Fei, C. Bertka, in *Mantle Petrology: Field Observations and High Pressure Experimentation,* Y. Fei, C. Bertka, B. Mysen, Eds. (Geochemical Society, Houston, TX, 1999), vol. 6, pp. 189–207.
25. X. Li, S. V. Sobolev, R. Kind, X. Yuan, C. Estabrook, *Earth Planet. Sci. Lett.* **183**, 527 (2000).
26. P. M. Shearer, T. G. Masters, *Nature* **355**, 791 (1992).
27. D. Bercovici, S. Karato, *Nature* **425**, 39 (2003).
28. R. Dasgupta, M. M. Hirschmann, *Nature* **440**, 659 (2006).
29. M. Akaogi, A. Tanaka, E. Ito, *Phys. Earth Planet. Inter.* **132**, 303 (2002).
30. P. Bird, *Geochem. Geophys. Geosys.* **4**, 1027 (2003), 10.1029/2001GC000252.
31. B. Steinberger, *J. Geophys. Res.* **105**, 11127 (2000).
32. We thank A. McNamara and J. Tyburczy for numerous discussions and helpful suggestions, and two anonymous reviewers for their comments. This work was supported by NSF grants EAR-0711401 (E.J.G.) and EAR-0453944 (N.S.) and by an Achievement Rewards for College Scientists Fellowship (N.S.).

The Impact of Agricultural Soil Erosion on the Global Carbon Cycle

K. Van Oost,[1]*†‡ T. A. Quine,[2]* G. Govers,[1] S. De Gryze,[3] J. Six,[3] J. W. Harden,[4] J. C. Ritchie,[5] G. W. McCarty,[5] G. Heckrath,[6] C. Kosmas,[7] J. V. Giraldez,[8] J. R. Marques da Silva,[9] R. Merckx[10]

Agricultural soil erosion is thought to perturb the global carbon cycle, but estimates of its effect range from a source of 1 petagram per year^{-1} to a sink of the same magnitude. By using caesium-137 and carbon inventory measurements from a large-scale survey, we found consistent evidence for an erosion-induced sink of atmospheric carbon equivalent to approximately 26% of the carbon transported by erosion. Based on this relationship, we estimated a global carbon sink of 0.12 (range 0.06 to 0.27) petagrams of carbon per year^{-1} resulting from erosion in the world's agricultural landscapes. Our analysis directly challenges the view that agricultural erosion represents an important source or sink for atmospheric CO_2.

Humans have drastically altered the global carbon cycle, mostly through increased use of fossil fuels and land use change (*1*). Global earth system models (*2*, *3*) represent well the changes in carbon flux between soil and atmosphere resulting from the reduced carbon inputs to soil and the accelerated decomposition of soil organic carbon (SOC) that accompany conversion of land from an undisturbed state to agricultural use (*4*, *5*). In contrast, the carbon dynamics of the well-documented acceleration of soil erosion and deposition (and resultant lateral fluxes of SOC) associated with conversion of land to agricultural use are poorly understood (*6*).

Soil erosion removes SOC from the site of formation and results in its burial in depositional environments. Recent analyses have identified three key mechanisms whereby these geomorphic processes, together or separately, may result in a change in the net flux of carbon between the soil and atmosphere (fig. S1). Mechanism M1 involves replacement of SOC at eroding sites as a result of continued inputs from plants and decrease in SOC available for decomposition (*6*, *7*); mechanism M2 is the deep burial of allochthonous and autochthonous carbon (*8*) and inhibited decomposition upon burial (*6*, *9*, *10*); and mechanism M3 is the enhanced decomposition of SOC as a result of the chemical or physical breakdown of soil during detachment and transport (*11*). The fundamental controls on the magnitude of the erosion-induced sink or source are then the rate at which SOC is replaced at sites of erosion, changes in the reactivity of SOC as a result of transport and burial, and the rates of soil erosion and deposition. Previous global assessments of the influence of erosion and deposition on carbon dynamics have made markedly different assumptions about these controls, resulting in the diametrically opposed assertions of a global net release or source of 0.37 to 1 Pg C year^{-1} (*12*, *13*) versus a net uptake or sink of 0.56 to 1 Pg C year^{-1} (*6*, *9*, *10*) as a consequence of erosion on agricultural lands.

The controversy about the role of erosion in the global carbon cycle reflects the inherent difficulty of quantifying a net flux controlled by interacting processes that are most often studied in isolation. We examined the integrated effect of the interacting processes using evidence for (i) the rate of SOC replacement at sites of erosion, (ii) the fate of the eroded and buried SOC within agricultural watersheds, and (iii) global soil erosion and soil carbon erosion rates (*14*). The first two lines of evidence were derived from a comprehensive large-scale survey of the SOC and caesium-137 (^{137}Cs) inventories (mass per unit area to given depth) of agricultural soils in Europe and the United States (table S1) that allows us to assess quantitatively the relationships between lateral and vertical SOC fluxes. We examined 1400 soil profiles from 10 watersheds (1 to 14 ha), including noneroded soils and eroding hill slopes as well as colluvial soils where sediment and SOC are buried. The artificial fallout radioisotope

[1]Physical and Regional Geography Research Group, Katholieke Universiteit Leuven, 3001 Heverlee, Belgium. [2]Department of Geography, University of Exeter, EX4 4RJ Exeter, UK. [3]Department of Plant Sciences, University of California, Davis, CA 95616, USA. [4]U.S. Geological Survey, Menlo Park, CA 94025, USA. [5]U.S. Department of Agriculture, Agricultural Research Service, Hydrology and Remote Sensing Laboratory, Beltsville, MD 20705–2350, USA. [6]Department of Agroecology and Environment, Research Centre Foulum, University of Aarhus, 8830 Tjele, Denmark. [7]Laboratory of Soils and Agricultural Chemistry, Agricultural University of Athens, 11855 Athens, Greece. [8]Department of Agronomy, University of Cordoba, 14080 Cordoba, Spain. [9]Instituto de Ciências Agrárias Mediterrânicas, Department of Rural Engineering, University of Évora, Évora, Portugal. [10]Division of Soil and Water Management, Katholieke Universiteit Leuven, 3001 Heverlee, Belgium.

*These authors contributed equally to this work.
†Present address: Département de Géographie, Université Catholique de Louvain, 1048 Louvain-la-Neuve, Belgium.
‡To whom correspondence should be addressed. E-mail: kristof.vanoost@uclouvain.be

Table 1. Watershed-averaged sediment and SOC budgets derived from the model simulations for the intermediate scenario. The rates are representative of the whole period of agricultural activities.

Site	Area (%)		Lateral sediment transfers (Mg ha⁻¹ year⁻¹)		Lateral SOC transfers* (g C m⁻² year⁻¹)		Vertical carbon transfers† (g C m⁻² year⁻¹)		Ratio vertical/ lateral carbon flux‡ (%)		
	Ero	Depo	Ero	Depo	Ero	Export	Ero	Depo	Min	Mean	Max
1	45	20	22.7	16.5	13.2	3.6	2.5	0.0	17	19	24
2	45	21	14.7	7.8	12.8	6.0	5.7	1.4	43	45	55
3	44	26	12.8	11.4	16.6	1.9	5.2	2.3	28	31	53
4	33	20	15.2	9.2	10.6	4.2	3.2	−1.1	27	30	42
5	47	35	13.4	11.3	10.1	1.6	2.4	−0.8	14	24	42
6	42	21	13.1	9.0	21.0	6.7	5.2	−0.7	11	25	39
7	39	22	6.4	3.5	6.2	2.8	1.6	−0.8	16	26	44
8	20	14	5.3	5.0	3.2	0.2	0.7	0.1	16	21	30
9	49	33	15.4	n.a.	32.2	n.a.	5.7	n.a.	11	18	22
10	47	34	13.4	n.a.	29.7	n.a.	5.7	n.a.	12	19	24
Average	41	25	13.2	9.2	15.5	3.4	3.8	0.05	19	26	38
Std	(±9)	(±7)	(±5)	(±4)	(±10)	(±2)	(±2)	(±1)	(±10)	(±8)	(±12)

*SOC erosion calculated as $Cw \cdot Ecs / 100$, where Cw is the carbon content (%) for the top layer and Ecs is the erosion rate (g m⁻² year⁻¹), both averaged over the watershed. SOC export is calculated as $Cw \cdot (Ecs\text{-}Dcs) / 100$, where Dcs is the deposition rate. †Positive values indicate a net flux to soils; negative values indicate a net flux to the atmosphere. ‡Ratio is calculated using the lateral and vertical fluxes from the eroding sites. The values are derived from a conservative (Min), intermediate (Mean) and extreme (Max) model scenario (14).
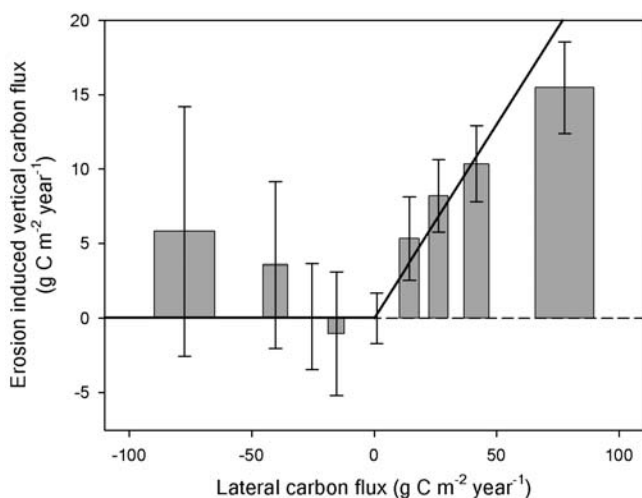
Fig. 1. Erosion-induced vertical carbon exchange between soils and atmosphere derived from 1400 profile measurements, grouped by lateral SOC fluxes (i.e., SOC erosion rates; positive values indicate erosion, negative deposition). SOC erosion is derived from the simulated SOC content (%) for the topsoil averaged over the watershed and profile-specific erosion rate derived from the ¹³⁷Cs data. Positive vertical exchange indicates a net flux to soils (sink); negative values indicate a flux to the atmosphere (source). The values are derived from the intermediate model scenario (14). The ranges of carbon erosion rates are −10 to 10, 10 to 20, 20 to 35, 35 to 50, and >50. Bar heights indicate mean values; error bars indicate 95% confidence intervals. Bars are centered on their median carbon erosion rate, and the width is proportional to their SD. The solid line represents the watershed-averaged relation (i.e., 26% and 0% replacement for the eroding and depositional areas, respectively; see Table 1).
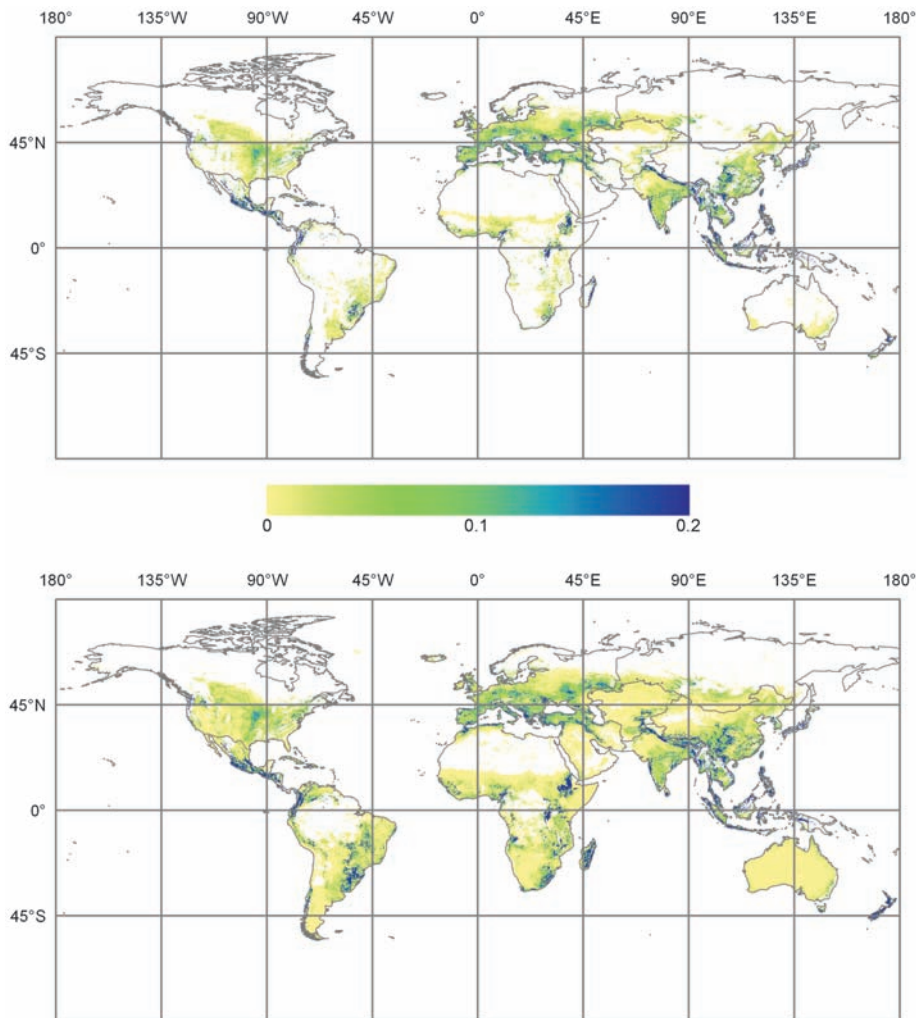
¹³⁷Cs was used as a tracer for soil material to determine rates of lateral soil transfer and the corresponding rates of subsoil excavation and soil burial relative to uneroded sites. The net vertical (soil-to-atmosphere) carbon flux associated with erosion and deposition was derived by establishing the difference between measured SOC inventories and SOC inventories simulated to result from lateral redistribution of SOC while assuming no net exchange of carbon between soil and atmosphere (15). The third line of evidence is provided by revised estimates of the contemporary global lateral fluxes of sediment and SOC in agricultural landscapes as a result of water and tillage erosion (the effect of wind erosion is not addressed). These estimates were derived using spatially explicit models of soil erosion in conjunction with global databases of land use, soil, climate, and SOC.

Mean rates of soil loss from the eroded areas in the 10 watersheds that we examined ranged from 4 to 23 Mg ha⁻¹ year⁻¹. These high rates of soil erosion were associated with rates of SOC export from the eroded areas that ranged from 3 to 32 g C m⁻² year⁻¹ (Table 1). The SOC budgets of all watersheds derived here (Table 1) are consistent with the operation of mechanism M1, in which the eroded areas of all 10 watersheds are found to act as sinks of atmospheric carbon, with a range of uptake from 1 to 6 g C m⁻² year⁻¹. This behavior is consistent with results of simulation studies (16–18) and with field data on the age of carbon and the presence of new carbon in eroding soil profiles (7). Despite large variability in climate, soils, and agricultural management, there is a correlation between sink strength and rates of SOC erosion found in the data for the 647 profiles subject to net erosion (Fig. 1). The average vertical:lateral flux ratio (carbon sink:SOC erosion ratio) is 0.26 (±0.08), whether derived using point data (Fig. 1) or integrated watershed data (Table 1, range of 0.11 to 0.55). The consistency of this proportion suggests that it can be used with predictions of lateral carbon fluxes (carbon erosion) to derive reliable estimates of sink strength under a wide range of climatic and management regimes. In deriving this proportion, we have taken into account site to site variations in the amount of subsoil SOC incorporated into surface horizons by erosion and variations in the SOC inventories. Furthermore, because only a fraction of the carbon exported from the eroded areas since the start of cultivation has been replaced by additional carbon derived from the atmosphere, the SOC inventories of eroding profiles have been subject to progressive depletion. The proportion of eroded SOC that is replaced is similar to the magnitude of the active SOC pool, which turns over within years to decades, and it seems probable that this pool undergoes most rapid replacement (19). The more passive pools accumulate as a result of a slow cascade of transformations, and both a longer period of time and a larger total throughput of SOC are required to replace these.

Although replacement of exported carbon at sites of erosion provides a sink of atmospheric carbon, the net effect of erosion and deposition on carbon exchange with the atmosphere is dependent on the fate of the SOC exported from the eroded areas. In the 10 sites examined here,

Fig. 2. (Top) Simulated global distribution of cropland SOC erosion by water and tillage. **(Bottom)** Simulated global distribution of agricultural carbon erosion (cropland + pasture- and rangeland) (Mg C ha^{-1} year^{-1}).

depositional environments found here are applied to the world's agricultural soils, the erosion-induced sink strength is ~0.12 Pg C year^{-1} (range 0.06 to 0.27) (22), of which 67% is accounted for by croplands.

The analysis presented here corroborates the hypothesis of an erosion-induced sink (6). However, our estimate is smaller than other estimates, which range between 0.56 and 1.2 Pg C year^{-1} (6, 9, 10). The reasons for this difference are twofold. First, global erosion rates have been overestimated in some studies because of a reliance either on aerial extrapolation of a limited number of plot experiments that are strongly biased toward steep slopes and fallow conditions (23) or on very coarse-grid implementation of hill slope erosion models (24, 25). Our approach, which explicitly accounts for watershed-scale processes at a very fine spatial resolution, yields erosion rates that reflect that most agriculture is situated on lowlands with relatively low relief intensities and consequently low erosion rates (26). Second, previous estimates were largely based on analysis of SOC stabilization in depositional environments and implicitly assumed that SOC contents were at steady state at eroded areas (i.e., 100% replacement of eroded SOC) (9, 10). We suggest that dynamic replacement of eroding carbon (6) is limited to the active carbon pools, which constitute on the order of 25% rather than 100% of the eroded carbon, and that this limits the magnitude of the atmospheric sink. Even the relatively modest sink that we derive may overestimate the true sink, because we have not accounted for decomposition losses from the exported SOC (21) and because the 26% replacement that we used is based on data from high-input agricultural systems, which may be less sensitive to yield decline than are low-input systems (27, 28).

Our analysis shows that vast quantities of sediment and SOC (0.47 to 0.61 Pg C year^{-1}) move laterally over Earth's surface as a result of agricultural erosion. The erosion conveyor excavates subsoil at eroding locations, transports it downslope through surface horizons, and buries former top-layer soil in depositional areas. Hence, both the spatial and vertical profile distribution of SOC in agricultural landscapes is continuously evolving, and carbon stock assessments based on topsoil sampling only is likely to result in erroneous interpretations and conclusions. Inclusion of tillage erosion, which is generally not included in studies of lateral SOC fluxes (16), substantially increased the flux as well as the area over which these processes take place. Our results indicate that over the past 50 years, globally, ~16 to 21 Pg C (29) have been buried within agricultural landscapes. However, the long-term stability of these pools under present and future climate disturbance remains highly uncertain (8, 30). The next steps in the quantification of the role of lateral SOC fluxes in the global carbon budget will require consideration for the potential increase in decomposition rates at sites of deposition as a

53 to 95% of eroded carbon was conserved and found to be redeposited within the watersheds over an area covering 14 to 35% of the watershed. This is consistent with earlier reports of the large amounts of retained erosion in watersheds (20).

In contrast to the areas of net erosion, the 256 profiles subjected to deposition show variation from a net source to a net sink (Fig. 1), with a watershed-averaged mean of 0 ± 1 g C m^{-2} year^{-1} (Table 1). These data suggest that preservation of buried carbon (mechanism M2) is effective and that, at the sites investigated, losses associated with transport (mechanism M3) are relatively minor. It appears that SOC redeposited within a short distance of the site of erosion, as in the sites examined here, is retained. Therefore, at the scale of the watershed/zero-order basin in which erosion and deposition occurs, the net exchange with the atmosphere is a sink, the magnitude of which is determined by the replacement of carbon at eroded locations with no measurable offset or additional contribution from the proximal depositional areas (6). The composite magnitude of

the sinks derived at this scale also sets the upper limit for the larger (landscape/regional) scale sink. However, it must be recognized that the fate of any SOC exported into the fluvial network and transported to distal depositional environments will determine the extent to which the landscape/regional scale sink magnitude approaches this upper limit (21).

On the basis of this analysis, the two most important controls on sink magnitude are identified as the rate at which SOC is eroded and the proportion of eroded SOC that is replaced at the sites of erosion. The last has been constrained by the analysis above. Using the models described in the (14), we estimate that the global contemporary agricultural sediment flux on cropland is about 22 Pg year^{-1} and that an additional approximately 11 Pg year^{-1} is mobilized on pasture- and rangelands (table S2). These sediment flux estimates correspond with a cropland SOC erosion rate of 0.32 Pg C year^{-1} and a total agricultural SOC erosion rate of 0.47 to 0.61 Pg C year^{-1} (Fig. 2). When the rate of SOC replacement on eroded soils and the reduced decomposition in

result of global warming, desiccation, land use change (*31*), and re-excavation by increased rates of water erosion (*24*), as well as the dynamics of SOC replacement at sites of erosion. Based on our analysis, we reject both the notion that agricultural erosion substantially offsets fossil fuel emissions and the view that agricultural erosion is an important source of CO_2.

References and Notes

1. R. Amundson, *Annu. Rev. Earth Planet. Sci.* **29**, 535 (2001).
2. A. Bondeau *et al.*, *Glob. Change Biol.* **13**, 679 (2007).
3. A. D. McGuire, *Glob. Biogeochem. Cyc.* **15**, 183 (2001).
4. J. Six, E. T. Elliott, K. Paustian, J. W. Doran, *Soil Sci. Soc. Am. J.* **62**, 1367 (1998).
5. E. A. Davidson, I. L. Ackerman, *Biogeochemistry* **20**, 161 (1993).
6. R. F. Stallard, *Glob. Biogeochem. Cyc.* **12**, 231 (1998).
7. J. W. Harden *et al.*, *Glob. Biogeochem. Cyc.* **13**, 885 (1999).
8. K. Yoo, R. Amundson, A. M. Heimsath, W. E. Dietrich, *Glob. Biogeochem. Cyc.* **19**, 917 (2005).
9. S. V. Smith, R. O. Sleezer, W. H. Renwick, R. Buddenmeier, *Ecol. Apll* **15**, 1929 (2005).
10. S. V. Smith, W. H. Renwick, R. W. Buddenmeier, C. J. Crossland, *Glob. Biogeochem. Cyc.* **15**, 697 (2001).
11. R. Lal, *Environ. Int.* **29**, 437 (2003).
12. P. A. Jacinthe, R. Lal, *Land Degrad. Dev.* **12**, 329 (2001).
13. R. Lal, M. Griffin, J. Apt, L. Lave, M. G. Morgan, *Science* **304**, 393 (2004).
14. Materials and methods are available as supporting material on *Science* Online.
15. T. A. Quine, K. Van Oost, *Global Change Biol.*, Online Accepted Articles, 10.1111/j.1365-2486.2007.01457.x (2007).
16. K. Van Oost *et al.*, *Glob. Biogeochem. Cyc.* **19**, GB4014 (2005).
17. S. G. Liu, N. Bliss, E. Sundquist, T. G. Huntington, *Glob. Biogeochem. Cyc.* **17**, 1074 (2003).
18. N. A. Rosenbloom, J. W. Harden, J. C. Neff, D. S. Schimel, *J. Geophys. Res.* **111 (G1)**, Art. No. G01004 JAN 31 (2006).
19. The proportion of eroded carbon being replaced at the eroding sites ranges from 0.11 to 0.55 when all errors are accounted for (Table 1). Based on radiocarbon studies of density separates (*32*) and bulk fractions (*33*) and on mass weights of SOC fractions (*34*) for globally diverse soils that are not generally eroded, the fraction of SOC that turns over within years to decades varies from 15 to 80%. Eroding sites are less studied, and carbon dynamics may be affected by the introduction of exposed subsoil, which is enriched with less reactive carbon substrates but may also provide nutrients for enhanced plant growth.
20. S. W. Trimble, P. Crosson, *Science* **289**, 248 (2000).
21. We note that burial of SOC in depositional environments has been shown to substantially reduce decomposition (*6*, *9*, *35*) and, therefore, carbon exported beyond watershed boundaries may be assumed to be protected from further decomposition. For our watersheds, the sink term is larger than the carbon export rate (Table 1), which suggests that erosion and deposition induce a sink, irrespective of the fate of the exported carbon.
22. We compared our global results with our high-resolution simulations at various spatial scales and established that our approach provides unbiased and scale-independent estimates of SOC erosion at the continental scale. The range is derived by using the 95% lower/upper confidence level of the replacement term (13 to 45%) using the conservative/extreme model scenario in combination with a low/high global SOC erosion estimate.
23. J. Boardman, *J. Soil Water Conserv.* **53**, 46 (1998).
24. A. Ito, *Geophys. Res. Lett.* **34**, L09403 (2007).
25. Supporting online text.
26. There is also indirect evidence that previous estimates of agricultural erosion are much too high. Estimates using data on river sediment load (*36*) estimated that human activities have led to an increase of ~2 Pg in the global river sediment flux to the ocean (if effects of large dams are omitted). Typical sediment delivery ratios for large basins is on the order of 10% (*11*), that is, an increase in global river sediment flux by 2 Pg should correspond to a global agricultural erosion rate on the order of 20 Pg, which is much more consistent with our estimates.
27. M. M. Bakker, G. Govers, M. D. A. Rounsevell, *CATENA* **57**, 55 (2004).
28. G. W. McCarty, J. C. Ritchie, *Environ. Pollut.* **116**, 423 (2002).
29. The range is obtained by multiplying the low/high global SOC erosion estimates for agricultural land by the average SOC export fraction obtained from our watersheds (30%) (Table 1).
30. K. Lorenz, R. Lal, *Adv. Agron.* **88**, 35 (2005).
31. A. A. Berhe, J. Harte, J. W. Harden, M. S. Torn, *Bioscience* **57**, 337 (2007).
32. S. Trumbore, *Glob. Biogeochem. Cyc.* **7**, 275 (1993).
33. K. Harrison, W. Broecker, G. Bonani, *Glob. Biogeochem. Cyc.* **7**, 69 (1993).
34. A. F. Plante *et al.*, *Eur. J. Soil Sci.* **57**, 456 (2006).
35. J. C. Ritchie, *Water Resour. Bull.* **25**, 301 (1989).
36. J. P. M. Syvitski, C. J. Vorosmarty, A. J. Kettner, P. Green, *Science* **308**, 376 (2005).
37. We thank R. Buddenmeier, S. Billings, A. Nicholas, W. Van Muysen, A. Berhe, and H. Van Hemelrijck for help and advice during the course of this work. Much of this work was supported by the European Commission under the Marie Curie IntraEuropean Fellowship Programme. The contents of this work reflect only the authors' views and not the views of the European Commission. K. Van Oost holds a postdoctoral position at the Fund for Scientific Research Flanders (FWO). J. Six and S. De Gryze were supported by the Kearney Foundation of Soil Science.

Why Is Climate Sensitivity So Unpredictable?

Gerard H. Roe* and Marcia B. Baker

Uncertainties in projections of future climate change have not lessened substantially in past decades. Both models and observations yield broad probability distributions for long-term increases in global mean temperature expected from the doubling of atmospheric carbon dioxide, with small but finite probabilities of very large increases. We show that the shape of these probability distributions is an inevitable and general consequence of the nature of the climate system, and we derive a simple analytic form for the shape that fits recent published distributions very well. We show that the breadth of the distribution and, in particular, the probability of large temperature increases are relatively insensitive to decreases in uncertainties associated with the underlying climate processes.

The envelope of uncertainty in climate projections has not narrowed appreciably over the past 30 years, despite tremendous increases in computing power, in observations, and in the number of scientists studying the problem (*1*). This suggests that efforts to reduce uncertainty in climate projections have been impeded either by fundamental gaps in our understanding of the climate system or by some feature (which itself might be well understood) of the system's underlying nature. The resolution of this dilemma has important implications for climate research and policy.

We investigate a standard metric of climate change: Climate sensitivity is defined as the equilibrium change in global and annual mean surface air temperature, ΔT, due to an increment in downward radiative flux, ΔR_f, that would result from sustained doubling of atmospheric CO_2 over its preindustrial value (2 × CO_2). It is a particularly relevant metric for current discussions of industrial emissions scenarios leading to the stabilization of CO_2 levels above preindustrial values (*2*). Studies based on observations, energy balance models, temperature reconstructions, and global climate models (GCMs) (*3–13*) have found that the probability density distribution of ΔT is peaked in the range $2.0°C \leq \Delta T \leq 4.5°C$, with a long tail of small but finite probabilities of very large temperature increases. It is important to ask what determines this shape and, in particular, the high ΔT tail, and to what extent we can decrease the distribution width.

Climate consists of a set of highly coupled, tightly interacting physical processes. Understanding these physical processes is a massive task that will always be subject to uncertainty. How do the uncertainties in the physical processes translate into an uncertainty in climate sensitivity? Explanations for the range of predictions of ΔT, summarized in (*14*), have focused on (i) uncertainties in our understand-

Department of Earth and Space Sciences, University of Washington, Seattle, WA 98195, USA.

*To whom correspondence should be addressed. E-mail: gerard@ess.washington.edu